Atmos. Chem. Phys. Discuss., 10, 15713–15753, 2010
www.atmos-chem-phys-discuss.net/10/15713/2010/
doi:10.5194/acpd-10-15713-2010

Atmospheric Chemistry and Physics Discussions

Quantifying immediate radiative forcing by black carbon and organic matter with the Specific Forcing Pulse

T. C. Bond[1], **C. Zarzycki**[1], **M. G. Flanner**[2], **and D. M. Koch**[3]

[1]Department of Civil and Environmental Engineering, University of Illinois at Urbana-Champaign, Urbana, IL, USA
[2]Department of Atmospheric, Oceanic and Space Sciences, University of Michigan, Ann Arbor, MI, USA
[3]NASA Goddard Institute for Space Studies, Columbia University, New York, NY, USA

Received: 18 May 2010 – Accepted: 26 May 2010 – Published: 28 June 2010

Correspondence to: T. C. Bond (yark@illinois.edu)

Published by Copernicus Publications on behalf of the European Geosciences Union.

Abstract

We propose a measure to quantify climate warming or cooling by pollutants with atmospheric lifetimes of less than one year: the Specific Forcing Pulse (SFP). SFP is the amount of energy added to the Earth system per mass of pollutant emitted. Global average SFP for black carbon, including atmosphere and cryosphere, is 1.12 $GJ\,g^{-1}$ and that for organic matter is $-0.061\,GJ\,g^{-1}$. We provide regional values for black carbon (BC) and organic matter (OM) emitted from 23 source-region combinations, divided between atmosphere and cryosphere impacts and identifying forcing by latitude. Regional SFP varies by about 40% for black carbon. This variation is relatively small because of compensating effects; particles from regions that affect ice albedo typically have shorter atmospheric lifetimes because of lower convection. The ratio between BC and OM SFP implies that, for direct forcing, an OM:BC mass ratio of 15 has a neutral effect on top-of-atmosphere direct forcing for any region, and any lower ratio induces direct warming. However, important processes, particularly cloud changes that tend toward cooling, have not been included here. We demonstrate ensemble adjustment, in which we produce a "best estimate" by combining a suite of diverse but simple models and enhanced models of greater complexity. Adjustments for black carbon internal mixing and for regional variability are discussed; regions with convection are implicated in greater model diversity. SFP expresses scientific uncertainty and separates it from policy uncertainty; the latter is caused by disagreements about the relevant time horizon, impact, or spatial scale of interest. However, metrics used in policy discussions, such as global warming potentials, are easily derived from SFP. Global-average SFP for biofuel and fossil fuel emissions translates to a 100-year GWP of about 760 for black carbon and −40 for organic matter when snow forcing is included. Ensemble-adjusted estimates of atmospheric radiative impact by black and organic matter using year 2000 emissions are $+0.46\,W\,m^{-2}$ and $-0.17\,W\,m^{-2}$, respectively; anthropogenic forcing is $+0.38\,W\,m^{-2}$ and $-0.12\,W\,m^{-2}$. The black carbon value is only 11% higher than that of the Intergovernmental Panel on Climate Change (IPCC), although this value includes enhanced absorption due to internal mixing.

ACPD
10, 15713–15753, 2010

1 Introduction

The atmosphere responds rapidly – within a few days or weeks – to the emission of short-lived climate forcers (SLCFs), such as aerosols or the precursors that result in ozone. Many of these SLCFs affect the Earth's radiative balance, either directly or by interacting with atmospheric chemistry. They also impact sensitive regions such as the Arctic (Quinn et al., 2008). Because mitigation of SLCFs could rapidly reduce climate warming, the possibility of decreasing them has engendered a flurry of interest (Hansen et al., 2000; Grieshop et al., 2009). However, the impact and the value of such reductions has been difficult to express. Global warming potentials (GWPs) are the currency of trading, and have been estimated for some short-lived species, but they do not communicate explicit information on rapid climate impact.

Here, we propose a measure of SLCF impact that does not rely on identifying the time horizon of interest, a question that lies outside of the purely scientific arena. It can be used directly to derive metrics desired by the policy community and to distinguish impact within a particular region of interest, such as the Arctic. In Sect. 2, we introduce the Specific Forcing Pulse (SFP). Section 3 presents regionally-specific values for black and organic carbon aerosol, derived using a single climate model. In Sect. 4, we move toward a "consensus" or "median" value based on model ensembles. Section 5 compares GWPs derived from this measure with previous estimates.

2 Impact measures

2.1 An instructive box model

Imagine a box (Fig. 1a) that represents a column of the atmosphere containing a first-order removal process with rate constant $1/\tau$. The integrated concentration over time of a pulse of pollutant species S_0 emitted into the box is τS_0. If the suspended pollutants capture energy per time per mass F (with a negative sign indicating energy rejection),

ACPD
10, 15713–15753, 2010

then the total added energy is ($\tau F S_0$), and the total added energy per emitted mass is (τF). This also happens to be the energy added per mass for continuous emission. A continuous emission rate E would result in a forcing (energy per time) of ($\tau F E$).

Emission rate (E), lifetime τ, and rate of energy capture per emitted mass (F, also called normalized forcing) are the major factors in climate forcing. Of course, in the atmosphere, τ, F, and E all vary in space and time. Nevertheless, their average global values can diagnose differences between models. Model studies commonly report measures such as column burden, forcing per mass, and total forcing; Fig. 1b shows the relationship between these basic measures and the box model parameters.

Total forcing is commonly reported by assessments such as the Intergovernmental Panel on Climate Change (IPCC, Forster et al., 2007), and this value depends on emission rate. One should examine varying forcing estimates in light of the emission inventory used, as that choice alone may account for the differences. Some estimates (Jacobson, 2001) include open biomass burning and should not be compared with forcing based on a subset of emission sources such as IPCC's fossil-fuel estimate of $+0.2\,\mathrm{W\,m^{-2}}$. IPCC's estimate of total black carbon forcing ($+0.34\,\mathrm{W\,m^{-2}}$) results from averaging models that use different emission rates; so the variation reflects disagreement about source strength as well as among model physics. Likewise, observationally-based estimates of forcing (e.g. Sato et al., 2003; Yu et al., 2006; Ramanathan and Carmichael, 2008) inherently include all emissions, not just those assumed in the model used. If observed and modeled forcing estimates differ, discrepancies could result from lifetime, normalized forcing, emissions, or some combination, and additional diagnosis is needed.

The policy-relevant measure is benefit, or disbenefit, per mass emitted – the "bang for the buck." By definition, this measure is independent of emission rate. It can be calculated by multiplying lifetime by normalized forcing (Fig. 1b), or by dividing total forcing by emission rate. Its physical interpretation is the amount of energy added to the Earth system during the emitted material's lifetime.

ACPD
10, 15713–15753, 2010

2.2 Specific Forcing Pulse

Compared with the time scales of interest in anthropogenic climate change, the perturbation of the Earth's radiative balance by a packet of emitted SLCFs effectively appears as a burst of energy. We propose that this energy (joules) added within a specific region, rather than power (watts, energy per time) or radiative forcing (watts per area), should be a fundamental measure. We call this measure the specific forcing pulse (SFP), defined for a species s as:

$$\mathrm{SFP}_s(A) = \int_0^A \int_0^{\tau=\infty} f_s(t,a) m_s(t,a) dt da \quad (1)$$

where f_s is the net change in energy flux per mass ($\mathrm{W\,m^{-2}\,g^{-1}}$ emitted), differing from F because it is normalized by area and may change with time after emission, m_s is the amount of the substance remaining at time t from a unit emission (g), a is a two-dimensional variable representing part of the Earth's surface, and A is the area of interest. The time horizon of interest, τ, is here chosen to be infinity and will be discussed below. Although forcing over a particular region may be isolated with Eq. (1), total global forcing should always be provided.

For a true pulse, the chosen time horizon has no effect; any choice ranging from a small Δt to infinity yields the same result. We argue that the term "pulse" may also be used when any reasonable choice of the upper time-integral limit yields an identical result. Further, we suggest that the minimum value of that limit is one year, as seasonal variations cause changes in f_s and m_s. This implies that species with e-folding lifetimes of four months or less (one-third of the shortest useful time horizon) may be treated as pulses for all realistic purposes.

SFP can be determined from the output of global climate models. It is the radiative forcing of each pollutant, integrated over the region and time period of interest (minimum one year), giving units of joules. The units of SFP are energy added to the Earth system per emission: joules per gram. This fundamental quantity can be used directly

ACPD
10, 15713–15753, 2010

in energy-balance approaches to the Earth system (e.g. Murphy et al., 2009). However, it is important to remember that forcing and warming are not the same; forcing is an input to the Earth system and does not account for its response. Just as instantaneous forcing cannot be divided by climate sensitivity to determine temperature change, SFP cannot be divided by the Earth's heat capacity to determine temperature change.

By convention, the term "forcing" in discussions about climate change has been defined as the net flux at the top of the atmosphere (TOA). We will present TOA values here unless otherwise identified, but we will also show that the concept of SFP can include other changes in energy flux.

This pulse concept is limited to climate forcers with relatively short lifetimes. For example, it is safe to say that CO_2 does not have a value of SFP. Its forcing during the first year after emission is less than 3% of the radiative forcing over 100 years. Thus, short-lived and long-lived impacts are very nearly orthogonal. Impacts of species with both short-lived and long-lived impacts, such as carbon monoxide, might be partitioned into two components: a pulse and an integrated forcing.

2.3 SFP and the absolute global warming potential

Another measure, the absolute global warming potential (AGWP), has the same basic calculation as the SFP. It has units of $\mathrm{W\,m^{-2}\,yr\,g^{-1}}$. This value, multiplied by annual emissions, was demonstrated by Forster et al. (2007). Its definition is:

$$\mathrm{AGWP}_s = \int_0^\tau f_s m_s(t) dt \tag{2}$$

SFP has some important differences from AGWP. First, SFP can refer to forcing within a specific region, although an exhaustive set of regions should always be provided to indicate total global forcing. This property requires that SFP be presented in conservative units of energy rather than forcing units. Except for this area-specific nature, SFP is a subset of AGWP, but it has some important differences in usage. Because it excludes long-lived pollutants, SFP is independent of time horizon, while AGWP is

ACPD
10, 15713–15753, 2010

not; the value of the latter remains ambiguous until a time horizon is given. SFP can be multiplied by emission rate to obtain annual forcing, while the same is not true of AGWP for longer-lived pollutants. SFP also expresses the immediacy of forcing change, while AGWP does not.

We have also chosen some different terminology. We avoid the term "global warming" because SFP is neither global nor required to produce warming. We identify the SFP as a "pulse" rather than a "potential" because it is not referenced to a chosen substance, as are global warming potentials and ozone depletion potentials.

2.4 SFP and the global warming potential

The currency of climate mitigation discussions is presently "carbon equivalence" using the global warming potential (GWP), which is defined as:

$$\mathrm{GWP}_s = \frac{\int_0^\tau f_s m_s(t)dt}{\int_0^\tau f_{CO2} m_{CO2}(t)dt} \tag{3}$$

If integration over the entire globe is assumed, then the numerator is both the AGWP and the SFP; the latter does not require a selection of time horizon. The denominator gives the amount of energy added to the Earth system by CO_2 during the time horizon τ.

The choice of time horizon reflects the value of future climate benefits. Current climate negotiations use τ=100 years, but others (e.g. 20 or 500 years) have been reviewed in public literature. That horizon matters only when some pollutant remains in the atmosphere at its end, as is the case for CO_2 but not for SLCFs. Vast differences in GWP for τ=20 years versus τ=100 years (Fuglestvedt et al., 2010) result entirely from the denominator, reflecting policy uncertainty. Including discount rates within the integrals is another method of assigning value to future climate change. This inclusion affects GWP of long-lived gases, but not of SLCFs. Even a very high discount rate of 10% alters the integral by less than 5% for a pollutant with a lifetime of 4 months.

ACPD
10, 15713–15753, 2010

Because the SFP involves no choice of time horizon, it avoids the value judgments inherent in choosing either a time horizon or a discount rate. Thus, SFP is a "science-policy handshake." It conveys the maximum physical information about a pollutant's interaction with the climate system, and makes the calculation of policy-relevant metrics easy, yet it can be based on purely scientific information.

A value of GWP can be obtained by dividing the SFP by a selected value for CO_2 integrated forcing. Using the Bern carbon model to represent life cycle, a_{CO2} from IPCC's Fourth Assessment Report (chp 2), and a zero discount rate for future forcing, the value of the denominator in Eq. (3) is 1.4×10^{-3} GJ g^{-1} for τ=100 years, and 4.0×10^{-4} GJ g^{-1} for τ=20 years.

2.5 Applications of SFP

A primary use of SFP is connecting decisions regarding mitigation and future emission with the resulting climate forcing. Because it represents forcing per emission, SFP can also be used to estimate immediate warming reductions caused by mitigating black carbon or ozone, or increased warming ("unmasking") due to sulfur controls. Integrated assessment models (Alcamo et al., 1994; Smith et al., 2000) can use the SFP to connect predictions of SLCF emission with radiative forcing.

Other measures have been proposed to examine mitigation decisions. These include the temperature response to a pulse emission (Shine et al., 2005; Fuglestvedt et al., 2010) or to a sustained emission cut (Boucher and Reddy, 2008). Both measures require assuming the "mitigation" emission rate as a function of time, as well as a baseline trajectory for comparison. The difference between the two trajectories is probably neither a pulse nor a constant. Instead, a measure that reflects the near-instantaneous forcing response to emissions is needed. The SFP can then be convolved with the time-dependent emission change [$e(t)$] and the temperature response function to a pulse emission, to obtain a temperature response to a particular measure, as was done by Boucher and Reddy (2008).

ACPD
10, 15713–15753, 2010

Because SLCFs are not well mixed throughout the atmosphere, locations of their concentrations, forcing, and deposition depend upon the emitting region (Berntsen et al., 2006). Furthermore, regional forcing does not indicate regional temperature response. Shindell and Faluvegi (2009) recently showed that Arctic temperature response depended on the forcing latitude, but in a non-intuitive way. As a first step in representing this complex situation, we propose the following equation:

$$\boldsymbol{I} = \int_0^{\tau} \mathbf{R} \cdot \boldsymbol{\varepsilon} \cdot \mathbf{SFP} \cdot \boldsymbol{e}(t) dt \quad (4)$$

where $\boldsymbol{I}$ and $\boldsymbol{e}$ are vectors in which the n-th element represents impact and emission, respectively, within region n; **SFP** is a matrix for which the m-th column and n-th row represent forcing in region n due to emission in region m; $\boldsymbol{\varepsilon}$ is a diagonal matrix representing a dimensionless efficiency of particular forcings; and **R** is a matrix for which the m-th column and n-th row give the response (temperature response or other chosen change) to forcing in region n.

We note that the term "efficacy" has been used in previous literature (Hansen et al., 2005) to denote the concept that is here conveyed by $\boldsymbol{\varepsilon}$. We also note that the "regions" in the equation could be smaller than the major regions presented in this paper, even as small as a city. However, uncertainties in atmospheric transport and impact may preclude such detailed divisions within SFP.

Equation (4) explicitly represents the process in transient climate models. Models are diverse in their forcing estimates and climate responses, but many models do not contain all elements of the equation; some represent forcing only, while some add climate response. Furthermore, a wide range of predicted future emission trajectories may exist. Identifying each component of the calculation from emission to climate response will allow a wide range of models to contribute to a final estimate of impact. Although Eq. (4) may not capture nonlinearities, we suggest that it is better than ignoring regional differences.

In this paper, we do not apply Eq. (4). We present it only to foreshadow the need for regional SFP, a discussion that will occupy the remainder of the paper.

ACPD
10, 15713–15753, 2010

3 Single-model, regional estimates of SFP

In this section, we present regionally-dependent values of the Specific Forcing Pulse for black carbon (BC) and organic matter (OM) particles. This concept could convey many changes in the radiative balance: warming or cooling of the atmosphere due to direct interaction with sunlight (*dir*); albedo changes in the cryosphere (snow and ice, *cry*); changes in warm clouds, and changes in cold or mixed clouds. We quantify only direct and cryosphere impacts here ($SFP_{TOA,dir+cry}$), noting that warm-cloud and cold-cloud changes could greatly alter the total.

3.1 Model description

We used the Community Atmosphere Model (CAM, Collins et al., 2006), developed at the National Center for Atmospheric Research, to model atmospheric and cryospheric (snow and ice) forcing by black and organic carbon. Atmospheric temperature and pressure were prescribed from NCEP re-analysis data, strongly constraining model winds. Energy-related emissions, from year 2000 in Bond et al. (2007), were 4400 Gg yr^{-1} and 8900 Gg yr^{-1} for black and organic carbon, respectively. Open-burning emissions from the Global Fire Emission Database, version 2 (van der Werf et al., 2006) averaged 2600 Gg yr^{-1} and 21 000 Gg yr^{-1} and included seasonality during each model year. Agricultural burning was not included because it appears in neither emission database. The emissions used here were later updated for the final forcing calculation. We provide forcing by organic matter – that is, material including associated hydrogen and oxygen – assuming that its mass is 1.4 times greater than that of organic carbon.

Aerosol optics were modified to reflect recent recommendations for black carbon (Bond and Bergstrom, 2006; Bond et al., 2006), including "coating" or internal mixing. This version of CAM does not have a full aerosol microphysical model, but the effects of coating can be approximated with higher absorption for black carbon particles that have aged. In our model, this transition has a characteristic time of about 1.2 days.

ACPD
10, 15713–15753, 2010

The organic matter in CAM has minimal absorption, ignoring the contribution of "brown" carbon, which has a small amount of absorption. It is less hygroscopic than sulfate, and therefore scatters less per mass. Model results are averaged over five years, after a discarded spin-up period of 4 months. This model produces global-average atmospheric forcing by black carbon from fossil fuels, biofuels, and open burning of $+0.40\,W\,m^{-2}$, and global-average forcing by organic matter of $-0.12\,W\,m^{-2}$.

Emissions from 23 separate region and source combinations (17 energy and 6 open burning) were tagged so that concentrations and deposition at each location could be attributed to source regions. The 17 regions reflect the groupings in a common integrated assessment model (IMAGE, Alcamo et al., 1994). We apportioned forcing in each model grid box ($1.9^{\circ} \times 2.5^{\circ}$) to the column burden of the aerosol from each region. Forcing through changes in ice and snow albedo was also modeled in a separate twenty-year equilibrium run (Flanner et al., 2009, run PD1). We apportioned this forcing to the 23 emitting regions using deposition of the tagged tracers. Global-average cryosphere forcing is $+0.047\,W\,m^{-2}$, with 20% of the total occurring in the Arctic. Figure 2 shows total forcing by BC and organic matter in the atmosphere, and BC on snow and ice.

3.2 Regional estimates of SFP for black and organic matter

Figure 3 shows $SFP_{TOA,dir,cry}$ for black carbon and organic matter emitted from the 23 region-sector combinations. BC has positive SFP (warming), while the negative SFP shows the cooling effect of reflective OM. There is more than an order of magnitude difference between the cooling per mass of OM and the warming per mass of BC; the latter is far more effective at interacting with visible radiation. For energy-related emissions, SFP of BC and OM averages +0.99 and $-0.030\,GJ\,g^{-1}$, respectively. Emissions from open burning have higher SFP_{TOA}: +1.13 and $-0.053\,GJ\,g^{-1}$ for BC and OM, respectively. Averages for all emissions are $+1.05\,GJ\,g^{-1}$ for BC and $-0.037\,GJ\,g^{-1}$ for OM.

ACPD
10, 15713–15753, 2010

The orange portion of each bar shows atmospheric impact at different latitudes, and the diagonally hatched portion represents energy added to the atmosphere within the Arctic (latitude 60–90° N). Energy added by instantaneous albedo changes (cryosphere forcing) is also shown as green bars. This forcing can also induce changes in snow and ice cover, a feedback that causes a higher temperature change per forcing that is greater for snow darkening than for CO_2 (Hansen and Nazarenko, 2004; Flanner et al., 2007). That feedback is not considered here.

Because the location of forcing matters to temperature responses in other regions (Shindell and Faluvegi, 2009), we have also partitioned SFP into latitude bands. Zonal transport is not well constrained and varies among models (Textor et al., 2006), so the divisions presented here should be treated as general guidelines rather than absolute separations. Unsurprisingly, dominant impacts are found at the same latitude as the region of emission.

Even with the lowest region (Japan) removed, there is a 40% difference among BC-SFP and a factor of 4 difference among OC-SFP for energy-related emissions. (Japan has a much lower SFP, but we neglect it because the emissions are small.) This variation, and the difference between energy-related and open-burning SFP, results from differences in normalized forcing (F) and aerosol lifetime (reflected in $m(t)$). Figure 4 shows the seasonality of normalized forcing for BC. For BC outside of the Arctic, the impact of emitted BC varies by 10–40% depending on the emitting region. This diversity results partly from the location of the aerosol; BC over a reflective surface has higher forcing per mass. Average normalized direct radiative forcing (NDRF) for extra-Arctic BC is about 40% higher in summer because the aerosol absorbs more sunlight during longer days, and because convection lofts the BC above reflective clouds. This convection also gives the aerosol a longer lifetime. This seasonality explains the higher SFP for open burning emissions, which are greater during summer, while energy-related emissions are nearly constant throughout the year.

For BC within the Arctic, warming per mass is also strongly seasonal and varies little by emitting region. Once aerosol arrives at the Arctic, its strong impact is governed

ACPD
10, 15713–15753, 2010

by conditions there, not by emitting region. Very little OM cooling occurs in the Arctic, because reflective OM over a bright surface has little effect on the radiative balance. Snow albedo increases SFP_{TOA} by about 15% on a global average. This contribution is important for, but not confined to, emissions in northern regions: Europe, the former USSR, and North America. Despite this cryosphere-forcing contribution, SFP in these regions is similar to that in more southerly regions. Cooler regions are closer to snow, but aerosols emitted from these regions have shorter atmospheric lifetimes due to lower convection.

3.3 Vertical energy distribution

Figure 5 also shows BC-SFP_{dir} for the 23 regions, this time showing the division between atmospheric heating, a positive forcing, and negative surface forcing. Top-of-atmosphere forcing is the sum of the two, and is identical to SFP_{TOA} in Fig. 3. The diversity of $SFP_{heating}$ among regions is similar to that of SFP_{TOA}, and biomass-burning BC again has a stronger impact per emission. The energy balance in Fig. 5 demonstrates the important impact of BC on redistribution of energy. Considering atmospheric impact alone, each gram of emitted BC adds about 1 GJ to the system when a boundary is drawn at the top of the atmosphere; it also heats the atmosphere by 2.4 GJ and prevents 1.5 GJ from reaching the surface. The surface energy budget is relevant to determining changes in the hydrologic cycle (Chung et al., 2002; Meehl et al., 2008).

4 Ensemble-adjusted models

There are two major sources of potential bias in our estimates of $SFP_{TOA,dir,cry}$. First, the model we used could be biased relative to other models. Second, all models could be biased relative to reality because of common, but incorrect, assumptions about aerosol representations. We address the first challenge here; a quantitative assessment of the second possibility is greatly needed.

ACPD
10, 15713–15753, 2010

The balance between multi-model "consensus" and detail is a common conundrum. Single models may contain needed features, such as diagnostics for regionally-specific SFP, or the inclusion of aerosol mixing which increases positive forcing. However, individual models may be prone to suspicion, so that model ensembles provide greater confidence. Because of the complexity of parameterizing global models, there may be a lag between observations that identify important processes, and the ability of most models to simulate those processes. Below, we outline a procedure to provide an "ensemble-adjusted" result that combines model results.

Assume that we begin with a "fully sensitive" model in which key processes can be turned on and off without changing any other model parameters, as discussed in the previous section. For each key process, we will refer to process-on simulations as "enhanced" model results, and process-off simulations as "baseline" results. We define E_{proc} as the enhancement by that process, or the ratio of enhanced to baseline SFP from each model. (The subscript may be changed to indicate the nature of the process.)

The best guess of SFP is:

$$\mathrm{SFP}_{\mathrm{best}} = \mathrm{SFP}_{\mathrm{full}} A_{\mathrm{tot}} \prod_i A_{\mathrm{proc},i} \tag{5}$$

where $\mathrm{SFP}_{\mathrm{full}}$ is obtained from the fully-sensitive model, and each A is an ensemble adjustment determined from all potential models. The total ensemble adjustment, A_{tot}, is the ratio between the mean or median of the baseline model ensemble and the baseline results of the fully-sensitive model. The process ensemble adjustment, A_{proc}, is the ratio between E_{proc} of the ensemble and E_{proc} of the fully-sensitive model. Each adjustment should have a central value and an uncertainty. E_{proc} should also be evaluated for consistency with "partly sensitive" models. A model might have implemented more than one process, so the net effect of a single process is not distinguishable. Or, that model might have implemented the process in a way that is less realistic than the fully sensitive models. Qualitative agreement among these comparisons might still indicate

ACPD
10, 15713–15753, 2010

confidence in E_{proc} and hence low variation in A_{proc}, or disagreement might suggest high uncertainty.

Our procedure is valid when key processes have multiplicative effects on the measure of interest (true for aerosol lifetime and normalized forcing). It also implies that the key process should be independent of other sources of model variability. If it is not, then correlations should be considered when assessing the overall uncertainty. Many factors affecting aerosol radiative forcing are not independent; for example, internal mixing can enhance both light absorption and CCN activity. For that reason, we evaluate uncertainties in SFP rather than in the components shown in Fig. 1.

It is frequently impossible to account for differing model treatments of all processes; the resulting variation will appear as an uncertainty in A_{tot}. The separate treatment of an individual key process using A_{key} is desirable when model representations are known to be biased and could be corrected, or when there is interest in exploring whether models agree on the effect of a key process.

Our proposed framework provides a more rigorous estimate from multiple models than does a simple average. In the sections that follow, we use the values of SFP determined in Sect. 3 as SFP_{full}.We first discuss the ensemble adjustment A_{tot} (Sect. 4.1). Section 4.2 discusses mixing between black carbon and non-absorbing aerosol components. This process increases absorption and positive forcing, yet many models do not consider it. We also discuss variability between regions (Sect. 4.3) and Arctic transport (Sect. 4.4) to investigate whether models agree on regional variability. Other model processes could be explored in this framework; for example, the hygroscopicity of organic matter affects both direct radiative forcing and cloud forcing. However, no results from fully-sensitive models are available to provide enhancement estimates, so variability resulting from this treatment remains in the model uncertainty A_{tot}.

4.1 Ensemble adjustment, A_{tot}

Baseline models will be those without black carbon mixing or diagnostics for regional variability. The AeroCom initiative organized multiple simulations with prescribed

ACPD
10, 15713–15753, 2010

emissions. Schulz et al. (2006) tabulated these simulations as well as previously published model results. The results without internal mixing form the baseline ensemble. We discarded values that were later superceded by the same research group, reasoning that if the individual researchers have moved beyond their early estimates, the community should too. The single model that included only clear-sky forcing is not included (Schulz et al., 2006) and our baseline SFP of $+0.57\,\mathrm{GJ\,g^{-1}}$ is added. The baseline ensemble includes models E, H, I, and L-S from Schulz et al. (2006). In addition, two models may have chosen relatively high mass absorption cross-sections for BC (UIO-GCM and SPRINTARS) in an attempt to account for internal mixing. These were adjusted downward by the ratio between the absorption cross-section for unmixed BC ($7.5\,\mathrm{m^2\,g^{-1}}$, Bond and Bergstrom, 2006) and the value used in the model. These models include only primary organic matter.

The baseline SFP from 12 models is shown as a frequency distribution in Fig. 6. Mean and median for BC are identical ($0.61\,\mathrm{GJ\,g^{-1}}$). For OM, the mean and median are -0.052 and $-0.049\,\mathrm{GJ\,g^{-1}}$, respectively. There is a factor of 13 difference between maximum and minimum, compared with a factor of four for BC. This greater disparity for OM may reflect a wider range of choices for water uptake and light absorption properties that affect forcing.

Figure 6 compares our baseline modeled SFP (red triangles) with the ensemble. It also shows the effect of the enhancement (red circle). Our baseline is similar to the median for BC and lower than the median for OM. The total ensemble adjustment is 1.03 for BC, and 1.30 for OC. Applying these to the enhanced value for BC results in a global average atmospheric SFP of $+0.96\,\mathrm{GJ\,g^{-1}}$. For OM, the global average is just the ensemble average, $-0.049\,\mathrm{GJ\,g^{-1}}$.

By magnitude, atmospheric BC outranks OM by a factor of 23 for energy-related burning, and 15 for open biomass. Thus, current models indicate that a OM:BC ratio of about 15, or an OC:BC ratio of about 11:1 leads to zero or positive top-of-atmosphere direct forcing. Any lower ratio has direct radiative warming, and the "neutral" ratio may be greater for some regions.

ACPD
10, 15713–15753, 2010

The coefficient of variation (standard deviation divided by mean) is 0.23 for BC SFP, and 0.60 for OM SFP. This is a first estimate of uncertainty. A better quantification is beyond the scope of this paper. To proceed further, the underlying causes of variation within models should be identified and evaluated with measurements, and models that more closely reproduce critical observations should be given a higher weighting.

4.2 Black carbon mixing: E_{mix} and A_{mix}

Mixing of black carbon with other aerosol components within individual particles ("internal mixing") increases absorption, and hence positive forcing, as first suggested by Ackerman and Toon (1981). This increase in absorption is not controversial. It has been confirmed in laboratory measurements (Schnaiter et al., 2005) and mixing occurs quickly after emission (Shiraiwa et al., 2007). The representation of mixing between black carbon and other species within single particles has been missing from many published model results. This situation is being rectified as aerosol models advance, but a full suite of upgraded model results is not yet available. Here, we examine only atmospheric forcing to determine E_{mix} and A_{mix} for the key process, aerosol mixing. To the best of our knowledge, our discussion here covers all published fully-sensitive model comparisons.

CAM simulations with and without mixed aerosol gave SFP_{dir} of +0.57 and +0.93 GJ g^{-1}, respectively (E_{mix}=1.6). This mixing enhancement is included in SFP_{full}. The purpose of the following discussion is a model comparison to determine whether the enhancement deserves a different adjustment. Other models suggest similar values of E_{mix}. Jacobson (2000), shows that core-shell particles result in an E_{mix} of two compared with the baseline case (0.76 versus 0.38 GJ g^{-1}). The greater enhancement in this model is qualitatively predictable. The baseline case used spherical particles that have less absorption, while uncoated particles in our baseline model had higher absorption because fresh black carbon particles are aggregates (Bond and Bergstrom, 2006). The ratio between absorption of mixed and unmixed particles in our enhanced

ACPD
10, 15713–15753, 2010

versus baseline runs is 1.5, while if unmixed particles were assumed to be spherical, the ratio would be about 1.8 (Bond et al., 2006). Chung and Seinfeld (2002) also examined mixed particles, although their particles were internally homogeneous instead of having a core-shell configuration. E_{mix} in their model was 1.6. Recent models based on measurements of particle morphology (Adachi et al., 2010) give lower values of E_{mix}, while models assuming the core-shell model with measured core and shell sizes (Moffett and Prather, 2009) suggest that E_{mix} could be even higher.

A recent model (Myhre et al., 2009) with an SFP of +0.99 GJ g^{-1} was not included in the ensemble because it included a lengthened aging time based on observed oxidation rates (Maria et al., 2004). This change increases the lifetime and hence the SFP, but tying aging to oxidation rates ignores the contributing of aging by coating, which is rapid (Moffett and Prather, 2009). Nevertheless, this research explored an aerosol mixing treatment similar to ours, resulting in a 27% increase in SFP. The lower increase in the new model is also qualitatively reasonable. The slower aging rate means that a greater fraction of aerosol is unaged and unmixed, so a mixing treatment increases the forcing less. We conclude that the increase in aerosol mixing in our model is reasonable. Although we can explain model differences qualitatively, because of the variation, we give A_{mix} a value of 1.0±0.2.

4.3 Regional diversity: E_{rgn} and A_{rgn}

Figure 3 shows differences in SFP_{dir} among regions. How robust are those regional differences? Here, we develop an ensemble adjustment for each region (A_{region}). Figure 7 compares the regional variation in BC atmospheric SFP between CAM and the four other models that show regional variation (Oslo-CTM, Berntsen et al., 2006, and Rypdal et al., 2009; GISS, Koch et al., 2007; MOZART, Naik et al., 2007; LMD, Reddy and Boucher, 2009). The "regional enhancement" shown in the figure (E_{rgn}) is the ratio between regional SFP and the most commonly reported value in regional studies: global-average SFP for energy-related emissions. Energy-related forcing values for the model of Naik et al. (2007) were not available for their most recent model version, so we

ACPD
10, 15713–15753, 2010

used a ratio to East Asian SFP derived from Saikawa et al. (2009; SFP=+0.95 GJ g^{-1}). Regional definitions are not identical in each model, so the comparisons are not exact. Reddy and Boucher (2007), Berntsen et al. (2006) and Rypdal et al. (2009) modeled only energy-related emissions, while Naik et al. (2007) examined only open burning.

For energy-related emissions in three regions (East Asia, North America, and Europe), the variation is low. The maximum and minimum values of E_{rgn} are within 15%. South Asia is different; the GISS model predicts very high regional enhancement, with the other models lying between GISS and CAM. In GISS and LMD, aerosol lifetime in South Asia is much higher than the global average, while CAM's lifetime is similar to the global average. Normalized forcing in the GISS model is similar to that in other regions. Thus, the high estimates from the GISS model are entirely due to aerosol lifetime, and the processes governing that lifetime should be constrained with observations. The available models, although limited in number, support the conclusion that SFP is relatively well-constrained in temperate regions – within about 20%. In tropical, convective regions, models differ in regional diversity, possibly due to parameterizations of convective removal and transport.

Regional enhancements are greater and more diverse for open burning emissions than for energy-related emissions. Temperate regions again agree better than tropical regions. CAM and MOZART agree that SFP is elevated above energy-related emissions at northern latitudes. In addition to convective removal, emission injection height could differ among models; GISS and CAM emissions are injected into the boundary layer. E_{rgn} from MOZART is much higher than that from CAM in South Asia and South America.

In Table 1, we combine the factors discussed above to provide estimates of $SFP_{atm,dir}$ by region. The overall ensemble adjustment (A_{tot}) of 1.03 is first applied to our regional SFP. Relative uncertainties of 0.23 for the ensemble adjustment, and 0.2 for mixing, apply to all regions. Uncertainties are assumed to be independent and are added in quadrature. Most of our regional SFP enhancements for energy-related combustion are within 10% of other models. An exception is South Asia (A_{rgn}=1.5). For

ACPD
10, 15713–15753, 2010

biomass burning, we apply regional adjustments to South Asia, South America, and Africa (A_{rgn}=1.4, 1.25, and 0.8, respectively). We choose uncertainties in A_{rgn} based on model diversity, with high uncertainties also applied when regions have not been studied: 15% for North America, Europe, and East Asia; 20% for Central and South America; 40% for South Asia, Middle East, and Africa. For open biomass burning in Europe, Northern Asia, and North America, we use a 15% uncertainty, while South Asia, South America, and Africa have a 40% uncertainty. The substantial uncertainties in the ensemble adjustment (A_{tot}) and optical properties (A_{mix}) create large uncertainties in regional SFP even when A_{rgn} is low. Finally, we weight regional SFP by emission rate to provide a global average SFP of 1.0 with an uncertainty of 40%.

Fewer studies are available for regional variations in OC (Berntsen et al., 2006; Naik et al., 2007; Koch et al., 2007). The studies broadly agree that SFP from South Asia, Africa and from biomass burning regions is of larger magnitude. Some unexplained factors include the slight positive SFP in Europe reported by Koch et al. (2007) and the factor of five to eight difference for biomass burning in Naik et al. (2007) as compared with that from East Asia by Saikawa et al. (2009) using the same model. Until these factors are sorted out, a true ensemble adjustment (A_{rgn}) is not possible. However, adjusting BC SFP and not OC SFP for regional differences, many of which are attributable to aerosol lifetime, could overstate positive forcing by an aerosol mixture. With some misgivings, we apply the same regional adjustments given above for BC to the values for OC.

4.4 Arctic transport and deposition

Poleward transport and removal of BC is particularly uncertain (Textor et al., 2006), affecting divisions between inside and outside of the Arctic in Fig. 3. If our transport to the Arctic were too low, then forcing there will also be too low. Uncertainties in snow albedo change also affect the cryosphere forcing in Fig. 4.

Figure 8 shows the diversity of predicted deposition in the Arctic from Shindell et al. (2008) compared with our model results (red dots). Deposition in our model is near

ACPD
10, 15713–15753, 2010

the ensemble median for North America and Europe, and comparatively low for aerosol from both East and South Asia. We use ensemble adjustment factors for spring, when impact is greatest (Flanner et al., 2007): 1.06 for North America and Europe, 1.3 for South Asia, and 2.4 for East Asia, applying these factors to the Arctic portion of cryosphere SFP only. In regions where CAM differs greatly from the median, the Arctic contribution is a small fraction of SFP: the ensemble adjustment for East Asia increases total SFP by only 2% and the change for South Asia is negligible. This transport may be a large uncertainty in Arctic radiative impact, but it is not a large uncertainty in global impact.

4.5 Total cryosphere forcing

Estimates of ice and snow forcing are more variable than those of atmospheric forcing. Koch et al. (2009) summarized cryosphere forcing estimates, which range from +0.01 to +0.16 $W\,m^{-2}$ and vary widely with the method of parameterization and the reference value of emission. Only one of the estimates is higher than +0.1 $W\,m^{-2}$, and that value has been superceded. The lowest estimate comes from a model (GISS) that compared 1995 forcing with 1890. In addition, feedbacks make the response to cryosphere forcing highly uncertain. Cryosphere forcing in CAM is +0.037 $W\,m^{-2}$ from fossil fuel and biofuel, and +0.047 $W\,m^{-2}$ when open biomass burning is added (Flanner et al., 2009). Total fossil and biofuel emissions produce +0.06 $W\,m^{-2}$ in GATOR-GCM (Jacobson, 2004; Jacobson, personal communication) and +0.03 $W\,m^{-2}$ in the GISS model. We conclude that the CAM values used for cryospheric SFP are in the mid-range, but the uncertainties are about 100%. Sensitivity analyses by Flanner et al. (2007) show that a few major model processes could easily result in such a large uncertainty.

ACPD
10, 15713–15753, 2010

5 Comparison with published measures

In this section, we translate SFP to forcing and global warming potential, as shown in Table 2. Regional values can be developed from Table 1 using the procedures outlined here. We compare those translated measures with other published values.

5.1 Global forcing

Total aerosol forcing is emission rate times SFP. Estimates of year 2000 energy-related emissions by Bond et al. (2007), plus updated emission factors, are 4.8 Tg BC and 15 Tg OM. These values of OM include a source-dependent OM-to-OC ratio. Multiplying these values by the average SFP for energy-related emissions (+1.08 and $-0.04\,\mathrm{GJ\,g^{-1}}$, respectively), converting units, and dividing by the area of the Earth gives $+0.32\,\mathrm{W\,m^{-2}}$ for BC (including cryosphere forcing) and $-0.035\,\mathrm{W\,m^{-2}}$ for OM. Likewise, we use SFP for open-burning emissions (+1.12 and $-0.071\,\mathrm{GJ\,g^{-1}}$) along with average emission rates from van der Werf et al. (2006) (2.6 Tg BC and 30 Tg OM). For open burning, we assume that organic matter is 1.4 times organic carbon for consistency with AeroCom emissions (Dentener et al., 2006). Forcing is $+0.19\,\mathrm{W\,m^{-2}}$ and $-0.13\,\mathrm{W\,m^{-2}}$ for BC and OM, respectively, from open-burning emissions. Table 2 summarizes these estimates and provides a breakdown between atmosphere and cryosphere.

IPCC (Forster et al., 2007) reports anthropogenic forcing, or the difference between present-day and an atmosphere with 1750 emissions. The net anthropogenic emissions given by Dentener et al. (2006) are: 4.2 Tg BC and 10.7 Tg OC from energy-related combustion, and 2.1 Tg BC and 21.9 Tg OC from open burning. These emissions result in anthropogenic forcing of $+0.43\,\mathrm{W\,m^{-2}}$ for BC and $-0.12\,\mathrm{W\,m^{-2}}$ for OC.

Our total aerosol forcing estimate of $+0.46\,\mathrm{W\,m^{-2}}$ for BC is higher than the $+0.34\,\mathrm{W\,m^{-2}}$ given by IPCC (Forster et al., 2007) for two reasons. First, we have not subtracted emissions from the year 1750; emissions may decrease below the 1750 value in the future regardless of whether they existed before the Industrial Revolution.

ACPD
10, 15713–15753, 2010

This increases BC forcing by +0.08 W m^{-2}. Second, we include the increased absorption caused by in-particle mixing (see Sect. 4.1) and exclude duplicate model results, but this increases BC forcing by only about +0.04 W m^{-2} because some models with mixing were already averaged in the IPCC's estimate. The increase in total forcing due to the snow contribution (+0.05 W m^{-2}) is smaller than IPCC's estimate because it includes new, more physically based studies.

Uncertainties in atmospheric forcing resulting only from the factors considered here (global and regional model diversity and black carbon mixing) are about 40% for atmospheric BC from energy-related combustion, and 50% for open burning. BC cryosphere forcing uncertainties are a factor of 2 in either direction. For OM, one standard deviation of model uncertainty is about 60%. These values do not include uncertainty due to emissions.

5.2 Global warming potential

Table 2 gives global warming potentials for black carbon and organic matter, calculated from SFP values in Table 1. GWPs for 100-year and 20-year time horizons are calculated by dividing SFP by 1.4×10^{-3} GJ g^{-1} and 4.0×10^{-4} GJ g^{-1}, respectively (see Sect. 2.2). Compared with previous estimates of GWP by our group (Bond and Sun, 2005), the global average value for atmospheric forcing is similar but slightly higher (710 vs. 680). Atmospheric GWP for energy-related emissions (fossil fuel and biofuel) is somewhat lower than for open burning (660 vs. 800).

Our atmospheric 100-year GWP for BC from energy-related emissions is about 30% higher than the global mean average calculated by Reddy and Boucher (2007) and Fuglestvedt et al. (2010), who provided values of 480 and 460, respectively. The difference occurs largely because their models did not include internal mixing of black carbon with other aerosol components. Fuglestvedt et al. (2010) used the same multi-model ensemble as we did, so their 100-year GWP for organic matter should be directly comparable. They provide a value of −69 for organic carbon; assuming that organic

ACPD
10, 15713–15753, 2010

matter (which includes oxygen and hydrogen) is 1.4 times organic carbon by mass, their value becomes −49. Ours is somewhat smaller (−40) because we excluded some early, superceded studies that assumed high hygroscopicity for organic matter.

Reddy and Boucher (2007) reported a very large warming contribution from snow albedo for European emissions – about a factor of two increase above atmospheric warming. This estimate is much higher than ours because they assumed a global average snow forcing of +0.1 $W\,m^{-2}$, a relatively high estimate. They also apportioned all snow forcing according to Arctic deposition of energy-related emissions, although much of the albedo impact is caused by open biomass burning (25%) and 80% of the remainder occurs outside of the Arctic. We find that adding snow forcing increases warming by atmospheric BC by only 20–25% for Europe. Other emissions, particularly energy-related emissions in the former USSR and open biomass burning in Siberia (N Asia), have much larger warming from snow deposition.

6 Conclusions, challenges, and caveats

In this paper, we compare modeled estimates for atmospheric and snow forcing of black and organic carbon, normalizing to emission rates. Our measure is a simple combination of model outputs, the Specific Forcing Pulse. It encapsulates the impact of a packet of emissions, either for a global total or within a region, and can be easily translated to other policy-relevant measures. We recommend a method of combining model diversity with model improvements to provide best estimates.

Global average SFP_{dir} for black carbon is 1.0±0.43 $GJ\,g^{-1}$ and that for organic matter is −0.050±0.025 $GJ\,g^{-1}$. These values translate to 100-year global warming potentials of 710 for BC and −40 for organic matter. Regional SFP varies by about 60% for black carbon and a factor of 4 for organic matter from energy-related combustion. Variation in open biomass SFP is greater because of the correlation between the seasonality of emissions and of convective lofting. The greater seasonality of open biomass burning results in a larger SFP compared with energy-related emissions, and therefore a higher

ACPD
10, 15713–15753, 2010

GWP. Twenty-year GWP for BC averages 2500, and that for OM is −150, also slightly greater than our earlier estimates.

Because of continuing interest in SLCFs and their mitigation, model estimates of total, sectoral or individual-source forcing are becoming common. To place new estimates in context of others' work, individual model results should always be accompanied by a comparison with model ensembles. Such comparisons should use normalized values, such as SFP, normalized forcing, or lifetime.

The SFP presented here incorporates model estimates of atmospheric and snow forcing. Future analysis should focus on two improvements, discussed below.

6.1 Cloud changes

Changes in aerosol emissions also causes differences in cloud albedo ("first indirect"), cloud lifetime ("second indirect"), and cloud amount due to atmospheric heating ("semi-direct"). Such changes often result in negative forcing (Chen et al., 2010; Koch and DelGenio, 2010), which would reduce the magnitude of the SFP for black carbon, and make that of organic carbon even more negative. There is a dearth of model studies examining cloud responses to emission changes, rather than total impacts. Such studies are needed before any measure, like the SFP, can incorporate this important change in forcing.

6.2 Incorporating observations

The possibility that all models could be incorrect is a serious one. Observational constraints and uncertainties should be embedded in the SFP. Not present in our discussion is a recent model estimate of very high atmospheric forcing by black carbon (Ramanathan and Carmichael, 2008). Their reported total forcing of $+0.9\,\mathrm{W\,m^{-2}}$ is higher than many other modeled estimates. However, because the estimate was partly based on observations, the large observed forcing could also result from actual emissions being higher than modeled emissions. Until the exact causes of difference are isolated,

ACPD
10, 15713–15753, 2010

such estimates cannot be used to provide an "impact-per-emission" measure like the SFP. However, the great difference from modeled values should serve as a caution that emissions, model processes, or both contain uncertainties not fully explored by global simulations.

Acknowledgements. This research was supported by the US EPA's Climate Office, the National Aeronautics and Space Administration under MAP (DMK) and NNG04GL91G (TCB), and by a UCAR ASP post-doctoral fellowship (MGF). Model runs were accomplished at the National Center for Atmospheric Research, sponsored by the National Science Foundation. We thank Steven J. Smith, John Bachmann, David Fahey, and Piers Forster for helpful comments. This paper has not been subjected to EPA's required peer and policy review and therefore does not necessarily reflect the views of the Agency. No official endorsement should be inferred.

References

Ackerman, T. P. and Toon, O. B.: Absorption of visible radiation in atmosphere containing mixtures of absorbing and nonabsorbing particles, Appl. Optics, 20, 3661–3667, 1981.

Adachi, K., Chung, S. H., and Buseck, P.: Shapes of soot particles and implications for their effects on climate, J. Geophys. Res., in press, 2010.

Alcamo, J., van den Born, G. J., Bouwman, A. F., de Haan, B. J., Klein Goldewijk, K., Klepper, O., Krabec, J., Leemans, R., Olivier, J. G. J., Toet, A. M. C., Vries, H. J. M. d., and Woerd, H. J. v. d.: Modeling the global society-biosphere-climate system: Part 2: Computed scenarios, Water, Air, Soil Pollut., 76, 37–78, 1994.

Berntsen, T., Fuglestvedt, J., Myhre, G., Stordal, F., and Berglen, T. F.: Abatement of greenhouse gases: does location matter?, J. Climate, 74, 377–411, 2006.

Bond, T. C. and Bergstrom, R. W.: Light absorption by carbonaceous particles: an investigative review, Aerosol Sci. Technol., 40, 27–67, 2006.

Bond, T. C. and Sun, H.: Can reducing black carbon emissions counteract global warming?, Environ. Sci. Technol., 39, 5921–5926, 2005.

Bond, T. C., Habib, G., and Bergstrom, R. W.: Limitations in the enhancement of visible light absorption due to mixing state, J. Geophys. Res., 111, D20211, doi:20210.21029/22006JD007315, 2006.

ACPD

10, 15713–15753, 2010

Bond, T. C., Bhardwaj, E., Dong, R., Jogani, R., Jung, S., Roden, C., Streets, D. G., Fernandes, S., and Trautmann, N.: Historical emissions of black and organic carbon aerosol from energy-related combustion, 1850–2000, Global Biogeochem. Cycles, 21, GB2018, doi:2010.1029/2006GB002840, 2007.

Boucher, O. and Reddy, M. S.: Climate trade-off between black carbon and carbon dioxide emissions, Energy Policy, 36, 193–200, 2008.

Chen, W.-T., Lee, Y. H., Adams, P. J., Nenes, A., and Seinfeld, J. H.: Will black carbon mitigation dampen aerosol indirect forcing? Geophys. Res. Lett., 37(9), L09801, doi:10.1029/2010GL042886, 2010.

Chung, C. E., Ramanathan, V., and Kiehl, J. T.: Effects of the South Asian absorbing haze on the northeast monsoon and surface-air heat exchange, J. Clim., 15, 2462–2476, 2002.

Chung, S. H. and Seinfeld, J. H.: Global distribution and climate forcing of carbonaceous aerosols, J. Geophys. Res., 107, 4407–4441, 2002.

Collins, W. D., Rasch, P. J., Boville, B. A., Hack, J. J., McCaa, J. R., Williamson, D. L., and Briegleb, B. P.: The formulation and atmospheric simulation of the Community Atmosphere Model Version 3 (CAM3), J. Climate, 19, 2144–2161, 2006.

Dentener, F., Kinne, S., Bond, T., Boucher, O., Cofala, J., Generoso, S., Ginoux, P., Gong, S., Hoelzemann, J. J., Ito, A., Marelli, L., Penner, J. E., Putaud, J.-P., Textor, C., Schulz, M., van der Werf, G. R., and Wilson, J.: Emissions of primary aerosol and precursor gases in the years 2000 and 1750 prescribed data-sets for AeroCom, Atmos. Chem. Phys., 6, 4321–4344, doi:10.5194/acp-6-4321-2006, 2006.

Flanner, M. G., Zender, C. S., Randerson, J. T., and Rasch, P. J.: Present-day climate forcing and response from black carbon in snow, J. Geophys. Res., 112, D11202, doi:11210.11029/12006JD008003, 2007.

Flanner, M. G., Zender, C. S., Hess, P. G., Mahowald, N. M., Painter, T. H., Ramanathan, V., and Rasch, P. J.: Springtime warming and reduced snow cover from carbonaceous particles, Atmos. Chem. Phys., 9, 2481–2497, doi:10.5194/acp-9-2481-2009, 2009.

Forster, P., Ramaswamy, V., Artaxo, P., Berntsen, T., Betta, R., Fahey, D. W., Haywood, J., Lean, J., Lowe, D. C., Myhre, G., Nganga, J., Prinn, R., Raga, G., Schulz, M., and Van Dorland, R.: Changes in atmospheric constituents and in radiative forcing, in: Climate change 2007: The physical science basis, edited by: Solomon, S., Qin, D., Manning, M., Chen, Z., Marquis, M., Averyt, K. B., Tigor, M., and Miller, H. L., Cambridge University Press, Cambridge, UK, 129–234, 2007.

ACPD
10, 15713–15753, 2010

Fuglestvedt, J. S., Shine, K. P., Berntsen, T., Cook, J., Lee, D. S., Stenke, A., Skeie, R. B., Velders, G. J. M., and Waitz, I. A.: Transport impacts on atmosphere and climate: Metrics, Atmos. Environ., in press, doi:10.1016/j.atmosenv.2009.1004.1044, 2010.

Grieshop, A. P., Reynolds, C. C. O., Kandlikar, M., and Dowlatabadi, H.: A black-carbon mitigation wedge, Nature Geosci., 2, 533–534, 2009.

Hansen, J. and Nazarenko, L.: Soot climate forcing via snow and ice albedos, Proc. Natl. Acad. Sci., 101, 423–428, 2004.

Hansen, J. E., Sato, M., Ruedy, R., Lacis, A., and Oinas, V.: Global warming in the twenty-first century: an alternative scenario, Proc. Natl. Acad. Sci., 97, 9875–9880, 2000.

Hansen, J., Sato, M., Ruedy, R., Nazarenko, L., Lacis, A., Schmidt, G. A., Russell, G., Aleinov, I., Bauer, M., Bauer, S., Bell, N., Cairns, B., Canuto, V., Chandler, M., Cheng, Y., Del Genio, A., Faluvegi, G., Fleming, E., Friend, A., Hall, T., Jackman, C., Kelley, M., Kiang, N., Koch, D., Lean, J., Lerner, J., Lo, K., Menon, S., Miller, R., Minnis, P., Novakov, T., Oinas, V., Perlwitz, J., Rind, D., Romanou, A., Shindell, D., Stone, P., Sun, S., Tausnev, N., Thresher, D., Wielicki, B., Wong, T., Yao, M., and Zhang, S.: Efficacy of climate forcings, J. Geophys. Res.-Atmos., 110, D18104, doi:18110.11029/12005jd005776, 2005.

Jacobson, M. Z.: A physically-based treatment of elemental carbon optics: implications for global direct forcing of aerosols, Geophys. Res. Lett., 27, 217–220, 2000.

Jacobson, M. Z.: Strong radiative heating due to the mixing state of black carbon in atmospheric aerosols, Nature, 409, 695–697, 2001.

Jacobson, M. Z.: Climate response of fossil fuel and biofuel soot, accounting for soot's feedback to snow and sea ice albedo and emissivity, J. Geophys. Res., 109, D21201, doi:21210.21029/22004JD004945, 2004.

Koch, D., Bond, T. C., Streets, D., Unger, N., and van der Werf, G. R.: Global impacts of aerosols from particular source regions and sectors, J. Geophys. Res., 112, D02205, doi:02210.01029/02005JD007024, 2007.

Koch, D., Menon, S., Del Genio, A., Ruedy, R., Alienov, I., and Schmidt, G. A.: Distinguishing aerosol impacts on climate over the past century, J. Climate, 22, 2659–2677, doi:10.1175/2008jcli2573.1, 2009.

Koch, D. and Del Genio, A.: Black carbon absorption effects on cloud cover, review and synthesis, Atmos. Chem. Phys. Discuss., 10, 7323–7346, doi:10.5194/acpd-10-7323-2010, 2010.

Maria, S. F., Russell, L. M., Gilles, M. K., and Myneni, S. C. B.: Organic aerosol growth mechanisms and their climate-forcing implications, Science, 306, 1921–1924, 2004.

ACPD
10, 15713–15753, 2010

Meehl, G. A., Arblaster, J. M., and Collins, W. D.: Effects of black carbon aerosols on the Indian Monsoon, J. Climate, 21, 2869–2882, 2008.
Moffet, R. C. and Prather, K. A.: In-situ measurements of the mixing state and optical properties of soot with implications for radiative forcing estimates, Proc. Natl. Acad. Sci., 106, 11872–11877, 2009.
Murphy, D. M., Solomon, S., Portmann, R. W., Rosenlof, K. H., Forster, P. M., and Wong, T.: An observationally based energy balance for the Earth since 1950, J. Geophys. Res.-Atmos., 114, D17107, doi:10.1029/2009jd012105, 2009.
Myhre, G., Berglen, T. F., Johnsrud, M., Hoyle, C. R., Berntsen, T. K., Christopher, S. A., Fahey, D. W., Isaksen, I. S. A., Jones, T. A., Kahn, R. A., Loeb, N., Quinn, P., Remer, L., Schwarz, J. P., and Yttri, K. E.: Modelled radiative forcing of the direct aerosol effect with multi-observation evaluation, Atmos. Chem. Phys., 9, 1365–1392, doi:10.5194/acp-9-1365-2009, 2009.
Naik, V., Mauzerall, D. L., Horowitz, L. W., Schwarzkopf, M. D., Ramaswamy, V., and Oppenheimer, M.: On the sensitivity of radiative forcing from biomass burning aerosols and ozone to emission location, Geophys. Res. Lett., 34, L03818, doi:10.1029/2006gl028149, 2007.
Quinn, P. K., Bates, T. S., Baum, E., Doubleday, N., Fiore, A. M., Flanner, M., Fridlind, A., Garrett, T. J., Koch, D., Menon, S., Shindell, D., Stohl, A., and Warren, S. G.: Short-lived pollutants in the Arctic: their climate impact and possible mitigation strategies, Atmos. Chem. Phys., 8, 1723–1735, doi:10.5194/acp-8-1723-2008, 2008.
Ramanathan, V. and Carmichael, G.: Global and regional climate changes due to black carbon, Nature Geosci., 1, 221–227, 2008.
Reddy, M. S. and Boucher, O.: Climate impact of black carbon emitted from energy consumption in the world's regions, Geophys. Res. Let., 34, L11802, doi:11810.11029/12006GL028904, 2007.
Rypdal, K., Rive, N., Berntsen, T., Fagerli, H., Klimont, Z., Mideksa, T. K., and Fuglestvedt, J. S.: Climate and air quality-driven scenarios of ozone and aerosol precursor abatement, Environ. Sci. Policy, 12, 855–869, doi:10.1016/j.envsci.2009.08.002, 2009.
Saikawa, E., Naik, V., Horowitz, L. W., Liu, J., and Mauzerall, D. L.: Present and potential future contributions of sulfate, black and organic carbon aerosols from China to global air quality, premature mortality and radiative forcing, Atmos. Environ., 43, 2814–2822, doi:10.1016/j.atmosenv.2009.02.017, 2009.
Sato, M., Hansen, J., Koch, D., Lacis, A., Ruedy, R., Dubovik, O., Holben, B., Chin, M., and

ACPD
10, 15713–15753, 2010

Novakov, T.: Global atmospheric black carbon inferred from AERONET, Proc. Natl. Acad. Sci., 100, 6319–6324, 2003.
Schnaiter, M., Linke, C., Möhler, O., Naumann, K.-H., Saathoff, H., Wagner, R., Schurath, U., and Wehner, B.: Absorption amplification of black carbon internally mixed with secondary organic aerosol, J. Geophys. Res., 110, D19204, doi:19210.11029/12005JD006046, 2005.
Schulz, M., Textor, C., Kinne, S., Balkanski, Y., Bauer, S., Berntsen, T., Berglen, T., Boucher, O., Dentener, F., Guibert, S., Isaksen, I. S. A., Iversen, T., Koch, D., Kirkevåg, A., Liu, X., Montanaro, V., Myhre, G., Penner, J. E., Pitari, G., Reddy, S., Seland, Ø., Stier, P., and Takemura, T.: Radiative forcing by aerosols as derived from the AeroCom present-day and pre-industrial simulations, Atmos. Chem. Phys., 6, 5225–5246, doi:10.5194/acp-6-5225-2006, 2006.
Shindell, D. T., Chin, M., Dentener, F., Doherty, R. M., Faluvegi, G., Fiore, A. M., Hess, P., Koch, D. M., MacKenzie, I. A., Sanderson, M. G., Schultz, M. G., Schulz, M., Stevenson, D. S., Teich, H., Textor, C., Wild, O., Bergmann, D. J., Bey, I., Bian, H., Cuvelier, C., Duncan, B. N., Folberth, G., Horowitz, L. W., Jonson, J., Kaminski, J. W., Marmer, E., Park, R., Pringle, K. J., Schroeder, S., Szopa, S., Takemura, T., Zeng, G., Keating, T. J., and Zuber, A.: A multi-model assessment of pollution transport to the Arctic, Atmos. Chem. Phys., 8, 5353–5372, doi:10.5194/acp-8-5353-2008, 2008.
Shindell, D. and Faluvegi, G.: Climate response to regional radiative forcing during the twentieth century, Nature Geosci., 2, 294–300, doi:10.1038/ngeo473, 2009.
Shine, K. P., Fuglestvedt, J. S., Hailemariam, K., and Stuber, N.: Alternatives to the global warming potential for comparing climate impacts of emissions of greenhouse gases, Clim. Change, 68, 281–302, 2005.
Shiraiwa, M., Kondo, Y., Moteki, N., Takegawa, N., Miyazaki, Y., and Blake, D. R.: Evolution of mixing state of black carbon in polluted air from Tokyo, Geophys. Res. Let., 34, L16803, doi:16810.11029/12007GL029819, 2007.
Smith, S. J., Wigley, T. M. L., Nakicenovic, N., and Raper, S. C. B.: Climate implications of greenhouse gas scenarios, Tech. Forecast Soc. Change, 65, 195–204, 2000.
Textor, C., Schulz, M., Guibert, S., Kinne, S., Balkanski, Y., Bauer, S., Berntsen, T., Berglen, T., Boucher, O., Chin, M., Dentener, F., Diehl, T., Easter, R., Feichter, H., Fillmore, D., Ghan, S., Ginoux, P., Gong, S., Grini, A., Hendricks, J., Horowitz, L., Huang, P., Isaksen, I., Iversen, I., Kloster, S., Koch, D., Kirkevåg, A., Kristjansson, J. E., Krol, M., Lauer, A., Lamarque, J. F., Liu, X., Montanaro, V., Myhre, G., Penner, J., Pitari, G., Reddy, S., Seland, Ø., Stier, P., Takemura, T., and Tie, X.: Analysis and quantification of the diversities of aerosol life cycles

ACPD
10, 15713–15753, 2010

within AeroCom, Atmos. Chem. Phys., 6, 1777–1813, doi:10.5194/acp-6-1777-2006, 2006.
van der Werf, G. R., Randerson, J. T., Giglio, L., Collatz, G. J., Kasibhatla, P. S., and Arellano Jr., A. F.: Interannual variability in global biomass burning emissions from 1997 to 2004, Atmos. Chem. Phys., 6, 3423–3441, doi:10.5194/acp-6-3423-2006, 2006.
Yu, H., Kaufman, Y. J., Chin, M., Feingold, G., Remer, L. A., Anderson, T. L., Balkanski, Y., Bellouin, N., Boucher, O., Christopher, S., DeCola, P., Kahn, R., Koch, D., Loeb, N., Reddy, M. S., Schulz, M., Takemura, T., and Zhou, M.: A review of measurement-based assessments of the aerosol direct radiative effect and forcing, Atmos. Chem. Phys., 6, 613–666, doi:10.5194/acp-6-613-2006, 2006.

ACPD
10, 15713–15753, 2010

Table 1. Ensemble-adjusted specific forcing pulse (SFP) for black carbon and organic matter.

	Black carbon SFP (GJ/g)			Organic matter	Rel. uncert.
	Atmosphere	Cryosphere	Total	SFP (GJ/g)	BC-atm
Average energy	0.93	0.15	1.08	−0.040	35%
Canada	0.79	0.37	1.16	−0.021	25%
USA	0.81	0.18	0.99	−0.030	25%
Central America	1.12	0.03	1.15	−0.052	40%
South America	1.17	0.02	1.18	−0.048	40%
Northern Africa	1.20	0.08	1.29	−0.058	60%
Western Africa	1.18	0.02	1.20	−0.061	60%
Eastern Africa	1.11	0.02	1.13	−0.067	55%
Southern Africa	1.21	0.01	1.22	−0.077	60%
OECD Europe	0.78	0.16	0.95	−0.032	25%
Eastern Europe	0.84	0.19	1.03	−0.036	30%
Former USSR	0.83	0.50	1.33	−0.030	30%
Middle East	1.14	0.17	1.31	−0.057	55%
South Asia	1.25	0.13	1.38	−0.080	65%
East Asia	0.82	0.18	1.00	−0.026	30%
Southeast Asia	0.93	0.01	0.95	−0.044	45%
Oceania	0.96	0.05	1.00	−0.055	50%
Japan	0.70	0.07	0.76	−0.014	35%
Average open	1.12	0.08	1.20	−0.070	55%
Europe	1.20	0.20	1.39	−0.071	40%
Northern Asia	1.42	0.59	2.01	−0.056	50%
Southern Asia	1.38	0.03	1.40	−0.094	70%
North America	1.47	0.37	1.84	−0.056	50%
S/C America	1.33	0.01	1.34	−0.090	65%
Africa	0.86	0.01	0.87	−0.060	45%
Global average	1.00	0.12	1.12	−0.061	

ACPD
10, 15713–15753, 2010

Table 2. Global average forcing and global warming potentials derived from SFP combined with estimates of emissions (aerosol and anthropogenic forcing) or carbon dioxide forcing (global warming potentials).

	BC atmosphere	BC atmosphere + cryosphere	Organic matter
Aerosol forcing ($W\,m^{-2}$)			
Global total	0.46	0.51	−0.17
Open biomass	0.18	0.19	−0.13
Energy-related	0.28	0.32	−0.035
Anthropogenic forcing with IPCC-AR5 emissions ($W\,m^{-2}$)			
Global total	0.38	0.43	−0.12
Open biomass	0.14	0.15	−0.10
Energy-related	0.24	0.28	−0.026
Global warming potential, 100-year			
Global average	710	760	−40
Average open biomass	800	860	−50
Average energy-related	660	770	−30
Global warming potential, 20-year			
Global average	2500	2700	−150
Average open biomass	2800	3000	−180
Average energy-related	2300	2700	−100

ACPD
10, 15713–15753, 2010

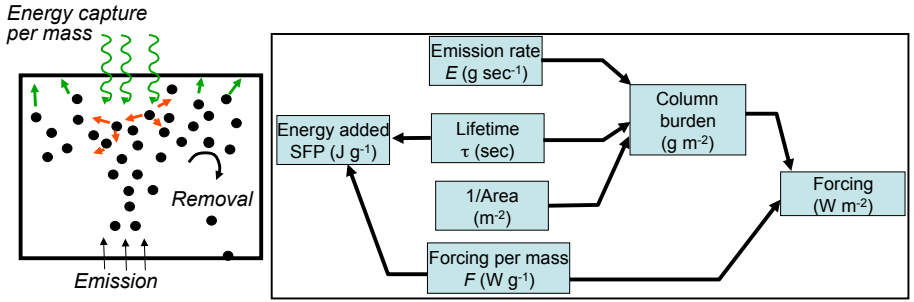

(a) Concept (b) Calculation

Fig. 1. (a) Simple box model of radiative forcing. Green arrows indicate incoming and rejected solar radiation; red arrows indicate capture and dissipation as heat. **(b)** Calculation flow, with arrows indicating multiplication (e.g., column burden = lifetime multiplied by emission divided by area). Energy added (specific forcing pulse) is an emission-independent measure of impact.

ACPD
10, 15713–15753, 2010

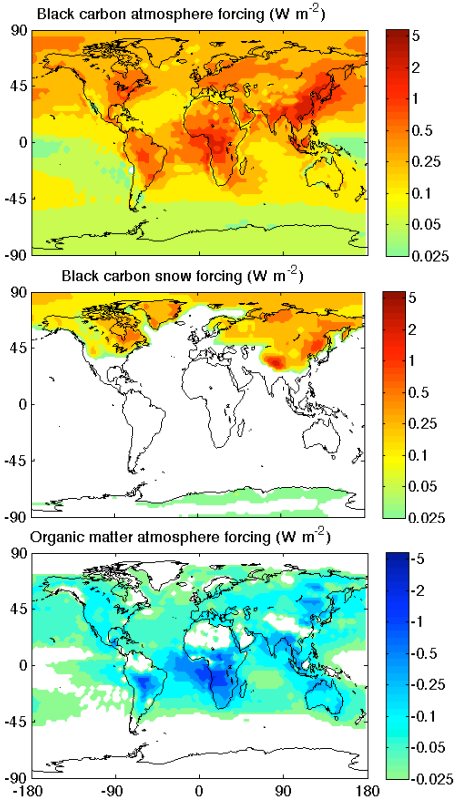

Fig. 2. Forcing by black carbon in atmosphere and on snow, and by organic matter, simulated with the Community Atmosphere Model.

ACPD
10, 15713–15753, 2010

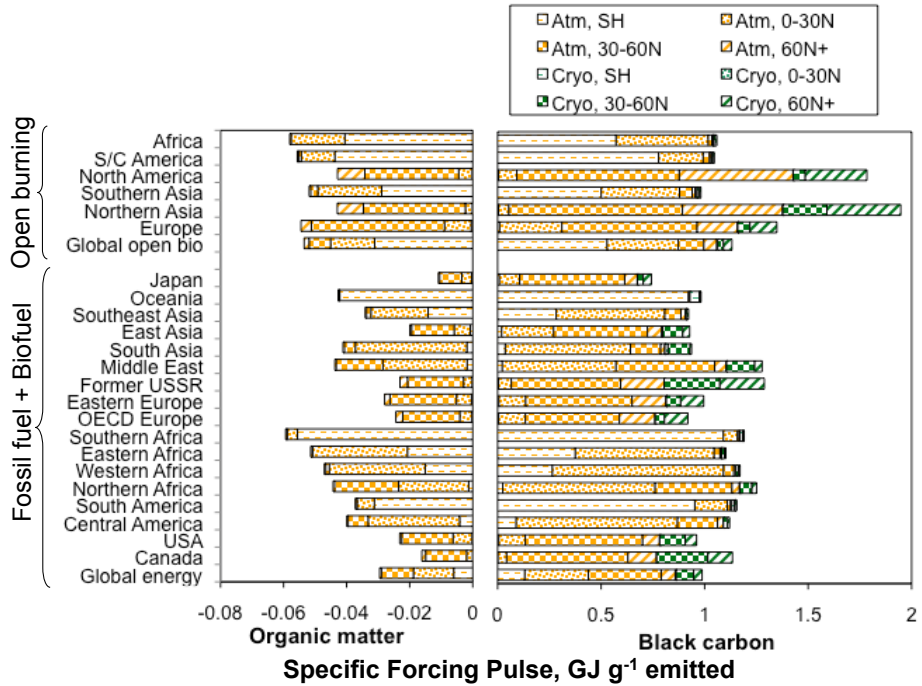

Fig. 3. Specific forcing pulse of aerosol emitted from 23 region-source combinations, estimated with a single model (NCAR CCSM). SFP includes direct atmospheric and cryosphere impacts only. Note the difference in scale between the positive values for black carbon and negative values for organic matter. These single-model values are adjusted according to model ensembles for a later table.

ACPD
10, 15713–15753, 2010

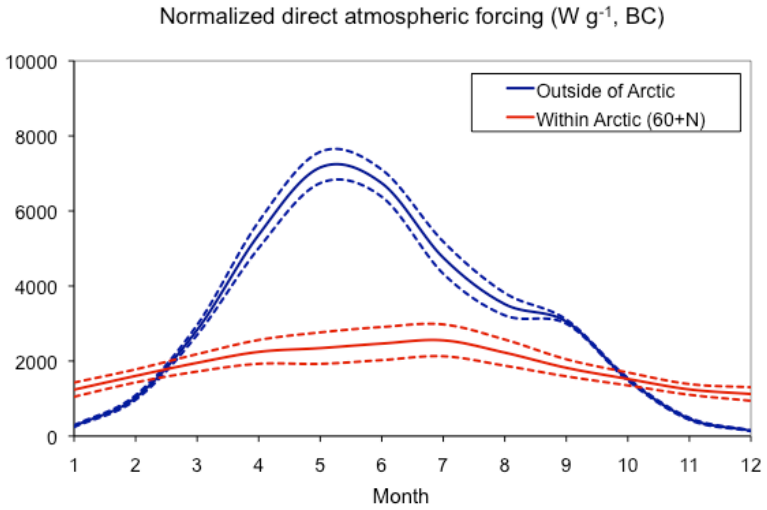

Fig. 4. Monthly normalized forcing for black carbon. Solid lines are global averages; dashed lines represent one standard deviation of the 23 emitting regions.

ACPD
10, 15713–15753, 2010

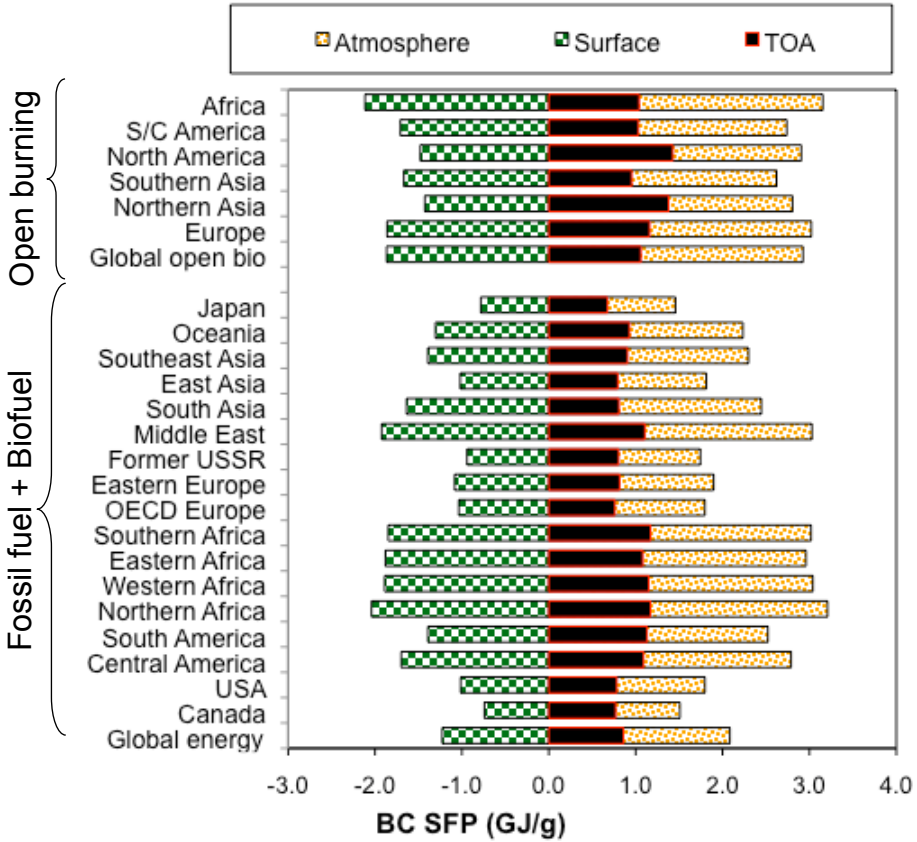

Fig. 5. SFP for black carbon, showing energy distribution. Energy is added to atmosphere (measured from zero), removed from surface. Top of atmosphere value, comparable to Fig. 3, is sum of surface and atmosphere.

ACPD
10, 15713–15753, 2010

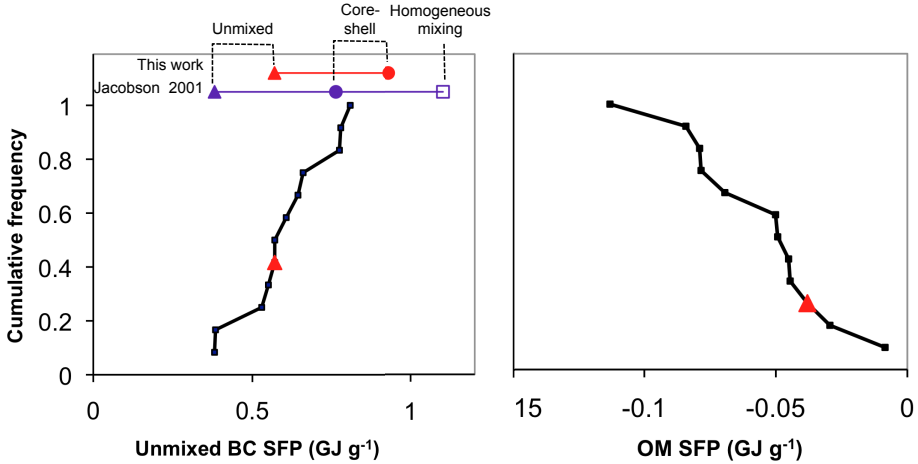

Fig. 6. Comparison of our baseline model results with AeroCom tabulation. Each figure shows SFP_{dir} derived from 12 models in the AeroCom tabulation, which reported normalized direct radiative forcing and aerosol lifetime. Red triangles indicate CAM results. Cumulative graphs indicate the fraction of models reporting SFP_{dir} below the indicated value. Figure for black carbon (left) also shows the effect of internal mixing from our model and one other.

ACPD
10, 15713–15753, 2010

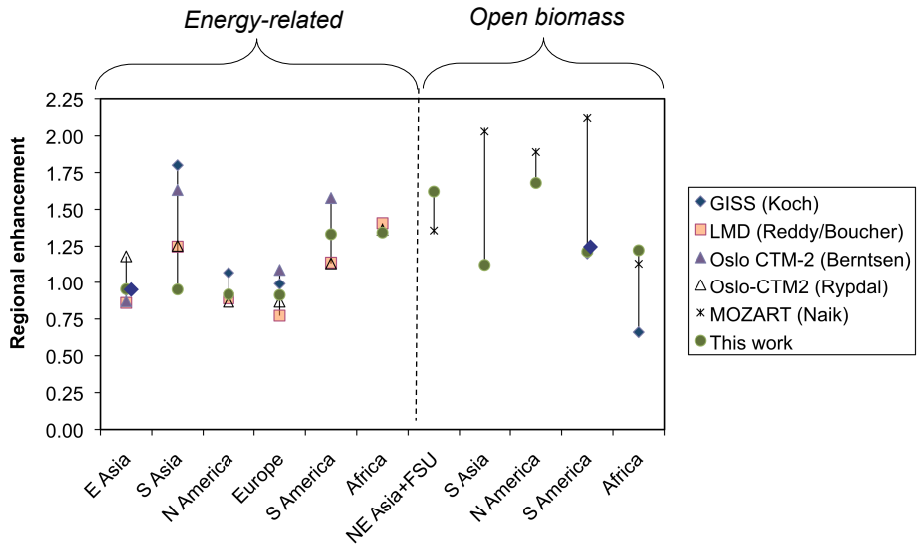

Fig. 7. Regional enhancement values for SFP_{dir} from four models. Regional enhancement is the ratio between regional SFP and global average energy-related SFP. Oslo CTM-2 did not provide global average values, so East Asia is used as a normalizing region, because its SFP is close to the global average in other models.

ACPD
10, 15713–15753, 2010

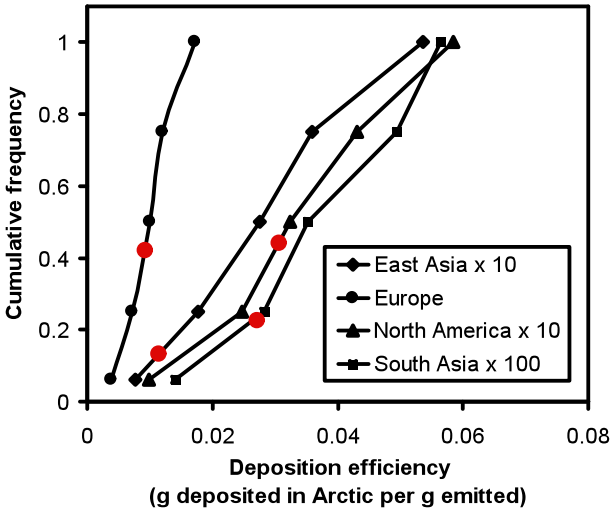

Fig. 8. Springtime Arctic deposition (March-April-May) from the model runs reported here (red dots) in context of model diversity (from Shindell et al., 2009).

ACPD
10, 15713–15753, 2010